Hindawi
Adsorption Science & Technology
Volume 2022, Article ID 3079663, 17 pages
https://doi.org/10.1155/2022/3079663

Review Article

Carbon-Based Materials as Effective Adsorbents for the Removal of Pharmaceutical Compounds from Aqueous Solution

Chian Ying Teo,[1] **Jim Sii Jack Jong**,[2] **and Yee Qian Chan**[2]

[1]*Department of Pharmaceutical Chemistry, School of Pharmacy, International Medical University, 57000 Kuala Lumpur, Malaysia*
[2]*Undergraduate, School of Pharmacy, International Medical University, 57000 Kuala Lumpur, Malaysia*

Correspondence should be addressed to Chian Ying Teo; teochianying@imu.edu.my

Received 23 April 2022; Revised 25 July 2022; Accepted 5 September 2022; Published 28 September 2022

Academic Editor: Walid Oueslati

Antibiotics are emerging water pollutants that have attracted significant attention from the scientific community. Antibiotics are generally released via hospital effluents, industrial production waste, animal manure, and irrigated agricultural land. Antibiotic residues can harm all living organisms, with the most detrimental consequence being the generation of antibiotic-resistant microorganisms, commonly known as "superbugs." Antimicrobial resistance is a concern to the healthcare community as it complicates the treatment of infections. Thus, the development of effective and economical technologies to remove antibiotics from the environment is necessary. Adsorption is a promising technology owing to its effectiveness and high operational feasibility, and carbon-based adsorbents are primitive materials that are particularly suited for antibiotic adsorption. Herein, an overview of the current state of antibiotic pollution will be summarised, including the adverse effects of different antibiotics and challenges associated with antibiotic removal. The adsorption behaviours of tetracycline (TC), quinolone, penicillin, and macrolides on carbon-based adsorbents (i.e., activated carbon, carbon nanotubes, and graphene-based materials) are reviewed. The interactions between antibiotics and carbon-based adsorbents, adsorption mechanism, and adsorption behaviour under different conditions are emphasised. In addition, the limitations of adsorption technology are highlighted to direct future research.

1. Introduction

Antibiotics are used to prevent and treat infectious diseases in humans and are extensively used in aquaculture and animal husbandry. [1] Antibiotic consumption has significantly increased, with reports that global antibiotic consumption rate increased 39% due to a rising defined daily dose of 65% between 2000 and 2015. [2] However, most antibiotics cannot be metabolised completely in humans and animals, allowing approximately 30 to 90% of the parent compounds to be discharged into the environment. [3, 4] Antibiotics have been detected in surface waters, groundwater, seawater, and soil. The dominant antibiotic residues of sulfonamides, macrolides, tetracycline (TC), and quinolones are detected in many surface waters. Table 1 shows the antibiotic residues detected in the aquatic environments of different countries. [4] The presence of excreted antibiotics in the aquatic environment promotes the development of antibiotic-resistant bacteria (ARB) and disturbs the ecological balance, posing an emerging threat to the ecosystem and human health [1, 3].

Recently, the spread of antibiotic resistance genes (ARGs) has rapidly increased along with the increase in antibiotic discharge into the environment. [1] ARGs persist in the environment and can be transferred between environmental bacteria and human pathogens. ARGs can eventually enter the food chain and affect human health. [1, 18] Antibiotic residues deteriorate drinking water quality by affecting the structural properties of metal ions. [19] Hence, the intake of antibiotic residues from the environment through eating and drinking has a potential biomagnification effect which may affect gut microbiota. It

Table 1: Antibiotic residues detected in the aquatic environments of different countries.

Antibiotics	Concentration (μg/L)	Country	Reference
Tetracycline	0.97	Canada	[5]
	0.11	United States	[6]
	48	United States	[7]
	2.31, 0.369, 0.706, 0.154, and 1.79	Portugal, Cyprus, Finland, Germany, and Norway	[8]
Oxytetracycline	1.34	United States	[6]]
Chlortetracycline	0.15	United States	[6]
Doxycycline	10	United States	[7]
	0.64	Sweden	[9]
Azithromycin	3.62, 2.99, 1.29, 1.26, and 1.49	Portugal, Spain, Finland, Germany, and Norway	[8]
Clarithromycin	0.74, 1.12, 0.045, 0.76, and 0.02	Portugal, Spain, Finland, Germany, and Norway	[8]
Erythromycin	3.9	United States	[7]
	1.6	Sweden	[9]
Tylosin	1.5	United States	[7]
Ciprofloxacin	0.119	Brazil	[10]
	0.03	United States	[11]
	0.657	Iran	[12]
	9.66	France	[13]
Norfloxacin	0.051	Brazil, United States	[11]
	0.09	Spain	[14]
Ofloxacin	0.34	Latin America	[15]
	17.1	Asia	[15]
	8.77	Spain	[13]
Amoxicillin	0.552	United Kingdom	[16]
Enrofloxacin	0.136	China	[17]

was reported that drug resistance-related diseases have caused >700,000 deaths per year, which may increase to 10 million per year by 2050 if the underlying causes are not addressed [4].

Conventional biological wastewater treatments are unable to remove antibiotic residues efficiently and require high energy consumption. [1, 2] Therefore, several antibiotic removal methods have been developed, including adsorption, ultrasonic cavitation, advanced oxidation technology, chlorination, electrochemical treatments, and membrane processes. [3] Adsorption is considered a particularly promising technology because of its ease of operation, high removal efficiency, universal application, and relatively low costs. [2, 3] This process can remove colour-forming organics, synthetic organic chemicals, heavy metals, and perchlorate. The interaction between the adsorbate and adsorbent is the driving force for capturing compounds of interest [4].

Various materials have been introduced for antibiotic removal from aqueous solutions, including carbon [20], polymeric materials [21], clay minerals [22], metals and their oxides [23], and chitosan [24]. Among these adsorbents, carbon materials have been widely applied to remove antibiotics because of their tunable surface functionalities, abundant pore structure, and high specific surface area. [25, 26] This review focuses on quinolone, penicillin, TC, and macrolide removal from aqueous solutions using carbon-based adsorbents including activated carbon as well as graphene-based, carbon nanotube-based, and biochar-based materials. The adsorption behaviour in terms of the mechanism, isotherm, and kinetics, along with influencing factors such as temperature and pH, is discussed herein.

2. Antibiotic Classes

Antibiotics are administered as therapeutics or prophylaxes to prevent and treat infections.[18] Antibiotics can be classified based on their chemical structure, mode of action, activity, administration route, and bacterial spectrum.[19] Antibiotics are commonly used in healthcare and veterinary medicine as inhibitors and biocides of infectious microorganisms. Additionally, they are used to raise livestock and as growth promoters in aquaculture, agriculture, and beekeeping.[3, 20] Antibiotic consumption has increased, and pathogen resistance to antibiotics has become a focal point of clinical and environmental research.[18] This paper will focus on TC, quinolone, penicillin, and macrolide antibiotics.

2.1. Tetracycline. TCs are broad-spectrum antibiotics derived from *Streptomyces aureofaciens* that are effective against Gram-positive and negative bacteria, allowing effectiveness against various bacterial infections.[3, 20] Based on their nature, elimination time, and dosage, TCs can be classified as TC, oxytetracycline (OTC), and chlortetracycline (CTC) [19], and their structures are shown in Figure 1. TCs are the most commonly used antibiotics worldwide because of their broad-spectrum activity, low toxicity, and low cost. [19, 22] However, they are

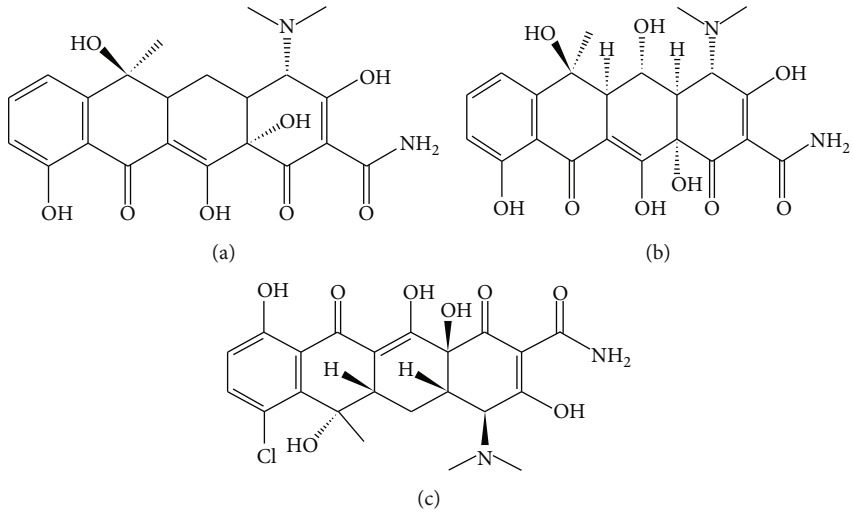

Figure 1: Structures of (a) tetracycline, (b) oxytetracycline, and (c) chlortetracycline.

unable to be metabolised completely in humans and animals. In addition, animal faeces as a plant fertiliser can lead to the notable persistence of residues in soil and aquatic environments.[21, 23] For example, the concentration of TCs detected in surface water in China was 482 ng/L, [20] while hospital wastewater exhibits TC concentrations of 100 μg/L and domestic wastewater contains concentrations closer to 1 μg/L. [19] In aquaculture farms in Malaysia, TC was most frequently detected (83%), with concentrations ranging from below the limit of quantification (LOQ) to 73 ng/L [24].

2.2. Quinolone. First-generation quinolones, including nalidixic acid (NDA) and cinoxacin, were discovered in the 1960s. [25, 26] The core chemical structure of the quinolone family is a bicyclic structure related to 4-quinolone (Figure 2). [26] The first-generation quinolones exhibit a narrow spectrum of activity and are effective against Gram-negative bacteria in the treatment of uncomplicated infections.[25] The major drawback of first-generation antibiotics is their high inhibitory concentration and low serum concentration when administered.[26] Therefore, a new generation of fluoroquinolones (FQs) was introduced. The addition of a fluorine atom at the R_6 position improved the activity spectrum and pharmacokinetic properties.[26] Ciprofloxacin (CIP), norfloxacin (NOR), and ofloxacin are well-known second-generation quinolones. To date, four generations of quinolones have been developed with activity against all Gram-negative organisms, including *Pseudomonas* sp. and Gram-positive organisms including *S. pneumoniae*, atypical pathogens, and anaerobic pathogens.[25] Newer quinolones are effective against various infections, including community-acquired pneumonia, intra-abdominal infections, pelvic infections, and sexually transmitted diseases.[25, 26] According to the review by Ahn et al., FQ is one of the five main classes of antibiotics detected in water samples from China, with a maximum concentration of up to 1000 ng/L [27].

2.3. Penicillin. The first antibiotic, penicillin, was discovered by Alexander Fleming in 1928 and has saved millions of lives by preventing and treating various infections. Penicillin protects against infections by inhibiting transpeptidase, a crucial enzyme for cell wall synthesis and maintenance.[28] The β-lactam ring is characteristic of the chemical structure for all penicillin antibiotics (Figure 3). Penicillin can be further divided into different categories according to substituents on the β-lactam ring.[28] First-generation penicillin, benzylpenicillin (penicillin G), is active against Gram-positive bacteria, including *Bacillus anthracis* and *Clostridium perfringens.* [28] Similar to quinolones, newer generation penicillins exhibit a broader spectrum with second-generation penicillin and amoxicillin (AMX) effective against Gram-negative rods, such as *Shigella*, *H. influenza*, and *E. coli*.[29] The development of fourth-generation penicillin (piperacillin) improved the spectrum activity against *Klebsiell*a and *Pseudomonas aeruginosa.* [28] A recent review reported the detection of AMX and penicillin in a river in China with a maximum concentration of 3380 ng/L [27].

2.4. Macrolide. Macrolides derived from *Streptomyces* are a class of weakly alkaline antibiotics which effective against Gram-positive and certain Gram-negative bacteria (Figure 4). Macrolide antibiotics include erythromycin (ERY), azithromycin, clarithromycin, tilmicosin, and tylosin. [3] The extensive use of macrolides in humans and animals poses a potential health risk due to bacterial resistance.[30] Azithromycin, clarithromycin, and ERY have been included in the European (EU) watch list of emerging concerns in the aquatic environment, [31] as they are frequently detected. For instance, up to 47 μg/L of ERY and roxithromycin was detected near swine farms and fishponds in the Haihe River Basin, China.[30] The presence of azithromycin with a concentration of 0.27 to 22.7 μg/L in municipal wastewater in the city of Zagreb has also been reported [32].

3. Antibiotic Pollution

TCs are not likely to cause acute toxicity, but chronic toxicity may occur in nontarget organisms that are exposed to antibiotics in the environment over extended periods. [33]

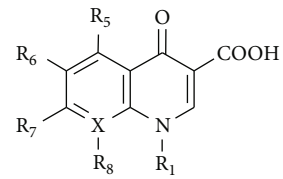

Figure 2: The general structure of quinolone.

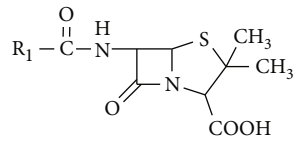

Figure 3: The general structure of penicillin.

TCs can persist in the environment because of their high hydrophilicity and low volatility, facilitating the production of ARGs. Additionally, the persistence of ARGs in drinking and irrigation water systems for agriculture poses a risk of infectious diseases by influencing the human intestinal microflora.[22] The presence of tet (O)- and tet (S)-mediated TC resistance in bifidobacteria has been reported, illustrating that the human gastrointestinal tract may serve as a reservoir of TC resistance genes [34].

In addition, FQ can be easily transferred to the soil because of its excellent chemical stability, modifying soil strains of *Salmonella typhimurium*. These modified bacterial strains are genotoxic and can cause DNA damage to aquatic organisms. In addition, morphological deformities of higher plants can result from photosynthetic pathway interference by accumulated FQ.[35] Furthermore, where animal manure is utilised as fertiliser in an agricultural setting, the chances of releasing antibiotic residues into the environment are increased. Lillenberg et al. discussed the possibility of plants adsorbing antibiotic residues from the soil, showing that FQs (CIP and NOR) could be detected in lettuce, common barley, and cucumber. [36] This suggested that antibiotics in the environment can be transferred to the edible parts of crops, leading to another antibiotic resistance route via food consumption.

AMX in the environment can negatively affect aquatic organisms, with a prominent example of catalase activity of *Danio rerio* being inhibited by exposure to a high AMX concentrations.[35] Once antibiotic residues enter the human body, they interact with the microbiome, and the intestinal microbiota often changes due to exposure to broad-spectrum antibiotics. For example, the composition of Firmicutes increases, while that of Bacteroidetes is reduced. [37] Diseases, including colorectal cancer, pseudomembranous colitis, and intestinal disorders, could arise from an imbalanced intestinal microbiome [38].

Lastly, the presence of macrolide residues in the environment may have harmful effects on humans and adverse effects on the environment. [31] Vestergaard et al. revealed that insufficiently treated effluent from azithromycin production resulted in enriched resistance genes to macrolide antibiotics in the receiving river. This results in a higher chance for a pathogen to capture these resistance genes, increasing the risk of humans being exposed to resistant pathogens via the food chain, recreational activities, and water intake. [39] In addition, tilmicosin was found to affect the development of zebrafish embryos, including cardiac congestion and causing teratogenic effects. Apoptosis and oxidative stress have also been observed in embryos exposed to tilmicosin [30].

4. Challenges Associated with Antibiotic Removal

Wastewater treatment plants that have been developed to remove pollutants, including nitrogen and phosphorus, are generally unable to effectively remove antibiotics and hormones. [40] Biological treatment has been widely used in wastewater treatment owing to its low environmental impact, high cost-effectiveness, and robustness.[41] Typical biological treatments included activated sludge, anaerobic digestion, photodegradation, fungal treatment, biosorption, biodegradation, and stabilisation.[4, 42] These methods typically depend on nematodes, bacteria, or small organisms to transform organic contaminants in wastewater into simple substances and to break down organic pollutants into biomass via normal cellular processes.[4] Nevertheless, several challenges remain for antibiotic removal from aquatic environments using conventional biological wastewater treatment.

Antibiotic removal is often hindered by their physicochemical properties. Volatility is an important property that is defined by the Henry's law constant (k_H), with k_H values of $> 3 \times 10^{-3}$ mol/(m^{-3}/Pa) indicating a molecule that is sufficiently volatile. However, antibiotics have relatively low k_H values of approximately $497 \times 10^{-31} - 158 \times 10^{-10}$ mol/(m^{-3}/Pa) and are difficult to remove via volatilisation.[43] High concentrations of solids suspended in wastewater increase the turbidity of the effluent, blocking sunlight from penetrating the top layer[42, 43] and limiting antibiotic photodegradation. The removal of antibiotics via biosorption depends on their hydrophobicity, which is usually measured using the octanol-water distribution (D_{OW}) or octanol-water partition (K_{OW}) coefficients. Compounds with high log D_{OW} (>3.0) and high log K_{OW} (>4.0) exhibit high adsorption on the solid phase.[43] Antibiotics with low adsorption potential have a lower removal rate than those with high adsorption potential. As representative examples, trimethoprim (log $K_{OW} = 0.73$) and ERY (log $K_{OW} = 2.48$) have lower adsorption potentials in sludge owing to their hydrophobicity [44].

In addition, antibiotic removal can be affected by operating conditions. Solid retention time (SRT) is a major factor that influences the removal of emerging pollutants from the aquatic environment, as it controls the diversity and size of the microbial community in wastewater. Generally, a high SRT value promotes microorganism proliferation in wastewater as well as increases and diversifies the microbial community.[42, 44] Enhanced removal of pharmaceutical compounds was found with an SRT of >26 days, whereas SRT of <8 days reduced removal efficiency. [44] Longer SRTs promotes slow-growing microorganism growth, including the nitrifying bacteria that are associated with antibiotic removal.[42] In addition, a short

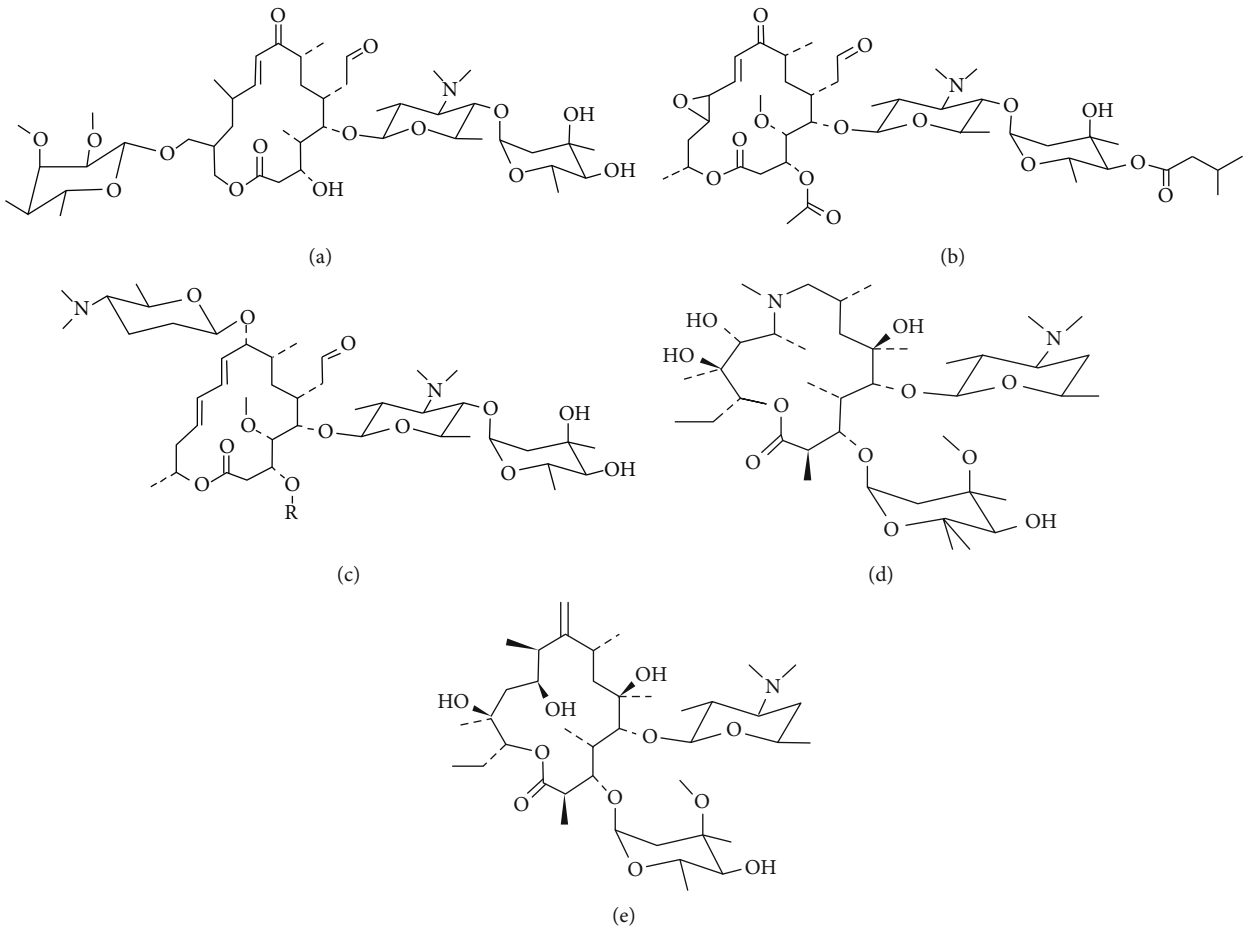

Figure 4: The structures of (a) tylosin, (b) carbomycin A, (c) spiramycin, (d) azithromycin, and (e) erythromycin [3].

SRT of <15 days was found to reduce the efficiency of the activated sludge due to reduced sludge availability [43].

The effect of pH on antibiotic removal performance is associated with the inherent properties of the antibiotics. Antibiotic molecules exist in different forms depending on the solution pH and the acid dissociation constants (pK_a) of the antibiotic. Therefore, pH changes affect the electrostatic interaction between sludge and antibiotics, which further affects the removal mechanism.[42, 43] For instance, electrostatic interactions govern the adsorption of FQ, macrolides, and TC in wastewater with a normal pH range of 6.5 to 7.5. [43] At pH 3.0 to 11.0, the surface charge of the biological sludge is predominantly negative, resulting in weak adsorption of sulfamethazine, which is anionic, due to electrostatic repulsion [45].

5. Different Approaches for Antibiotic Removal

Antibiotic removal approaches can be broadly categorised as biological, chemical, or physical. Biological treatments rely on live organisms, including bacteria and nematodes, to break down organic pollutants through biological processes.[4] The biodegradability of antibiotics is a major aspect to be considered, as only biodegradable antibiotics can be successfully removed through biological techniques.[4, 41] A simple closed-bottle test is typically conducted to estimate the biodegradability of antibiotics. According to the Organization for Economic Co-operation and Development (OECD), an antibiotic is considered biodegradable when oxygen demand in the testing vessel is 60% higher than the theoretical value for 28 days.[4] The efficiency of antibiotic removal through anaerobic processes was investigated, showing a higher percentage of AMX (~80%) was removed compared to CIP and enrofloxacin (~38%).[46] This is likely because FQ biodegradability is lower than that of penicillins, so biological treatments are considered less effective at removing antibiotics with poor biodegradability.

Chemical treatments involve altering the chemical structure of pollutants via oxidation, reduction, electrolysis, or catalysis. By altering the chemical structure, chemical properties such as solubility and volatility can be changed to reduce the ability of pollutants to remain in the aqueous system[4]. Chlorination is the most conventional technique used in drinking water systems because of its cost-effectiveness. Various chlorine species, including hypochlorite, chlorine gas, and chlorine oxide, have been used in this process. Chlorine oxide is preferred over other species because of its selectivity and ability to react with micropollutants, while preventing the formation of carcinogenic trihalomethane by-products.[47] Navalon et al. investigated the antibiotic removal properties of chloride oxides at different pH values, showing that chloride oxide could oxidise AMX and cefadroxil, but not penicillin G.[48] However, with decreasing pH, the oxidation reactivity with penicillin was enhanced,

while the reactivity with AMX and cefadroxil decreased because their chemical structures were altered by the varying pH. Chlorine oxide reacted with pollutants containing phenolic and tertiary amino groups, but not with molecules with functional groups including aromatic, hydrocarbons, 1° and 2° amine, aldehyde, and ketone groups.[49, 50]

Advanced oxidation is an alternative to conventional oxidation with chlorination that produces an extremely reactive hydroxyl radical (OH^-). Hydroxyl radicals have a higher standard oxidation potential ($E^o = 2.8$ V) than other oxidants, allowing them to oxidise most organic compounds.[47] Ozone (O_3) and hydrogen peroxide (H_2O_2) are typically used to produce radicals to oxidise pollutants into less toxic substances including carbon dioxide, water, or salts.[4, 47] Various techniques, including Fenton oxidation, ozonation, photocatalysis, and electrochemical processes, are considered advanced oxidation processes. Although the efficacy of advanced oxidation processes is high, its high cost is an undeniable disadvantage.

Physical treatments involve the removal of pollutants by van der Waals forces, hydrogen bonding, and dipole interactions.[4, 47] The reactant chemical structure is not altered during physical treatment and instead, in processes such as filtration, agglomerates form causing the physical state changes. [47] Other physical treatments include adsorption, filtration, coagulation, membrane treatment, and sedimentation.[4] The difference between physical and biological/chemical treatments is that physical treatment often does not involve pollutant breakdown. Instead, pollutants either separated or coagulated in a more concentrated form.[47]

Adsorption is the most commonly applied technique for removing pollutants because of its high capacity and design simplicity. It has been commonly applied as an efficient, effective, and economical technique for pollutant removal from wastewater for decades.[51] This process involves the mass transfer of chemical substances from the liquid phase to the solid phase. [4, 47] An advantage of adsorption over other techniques is that it does not produce secondary toxic by-products. Commonly used adsorbents are activated carbon (AC), graphene-based materials, and carbon nanotubes (CNTs).

6. Carbon-Based Adsorbents for Antibiotic Removal

To date, various adsorbents have been developed, and carbon-based adsorbents have been acknowledged as effective adsorbents for pollutant removal because of their high specific surface areas, strong interactions, and abundant pore structures. Common carbonaceous materials for antibiotic removal include AC, CNTs, graphene, and their composites (Figure 5). [52] The adsorption process and adsorption efficiency are greatly affected by the functional groups (-COOH, -OH, and $-NH_2$) in carbon-based adsorbents. Electrostatic interactions involving attraction between the adsorbents and an oppositely charged adsorbate are the primary adsorption mechanism between AC and antibiotics. Furthermore, hydrophobic interactions, $\pi - \pi$ interactions, $\pi - \pi$ electron donor-acceptor (EDA) interactions, and hydrogen bonds play prominent roles in the adsorption of antibiotics by carbon-based adsorbents (Figure 6). [52] The antibiotic removal efficiency, mechanism of interaction, and adsorption characteristics of the adsorbents are further discussed in the following sections.

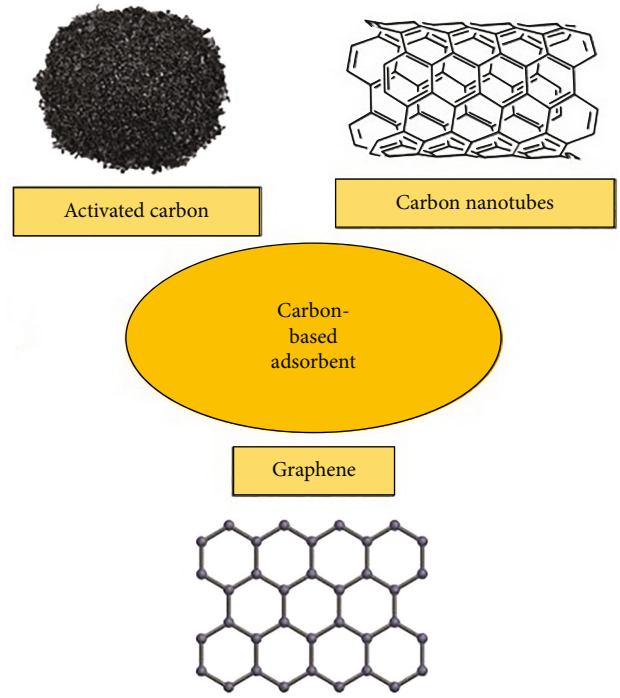

Figure 5: Carbon-based adsorbents. Activated carbon, carbon nanotubes, graphene, and their composites are common carbonaceous materials that show good adsorption capability for antibiotic pollutant removal.

6.1. Activated Carbon. AC is an activated black carbonaceous solid material with a large surface area, desirable pore-size distribution, and high adsorptive capacity. [23, 52] AC is a popular adsorbent used for the industrial-scale purification of water and air. Almost all carbon-based materials can be used to produce AC, but its properties depend on the material and activation method used. [3] Conventionally, AC is produced from petroleum, coal, lignite, and coke.[4, 52] Recently, different materials have been used to produce AC, including durian shells, coconut shells, olive stones, and wood.[53–56] Biochar (BC) and hydrochar (HC) have gained significant attention from researchers as alternative adsorbents to replace conventional activated carbon.[57] BC is a carbonaceous material produced via slow pyrolysis of biomass in an anoxic environment. HC is produced through hydrothermal carbonisation (HTC), a process wherein biomass is heated anaerobically in the presence of water.[57, 58] The difference between BC and HC is that dried biomass is used in the production of BC, whereas both dried and nondried biomass can be used in HTC [58].

Generally, differentiating between AC, BC, and HC causes confusion. Both BC and HC can be classified as AC after process "activation" where common activation methods for AC preparation can be classified as physical or chemical. During physical activation, the precursor material is activated after carbonisation at temperatures between 800 and 1000°C to prevent carbon losses. Chemical activation involves mixing activating agents with the raw material, followed by heating under an

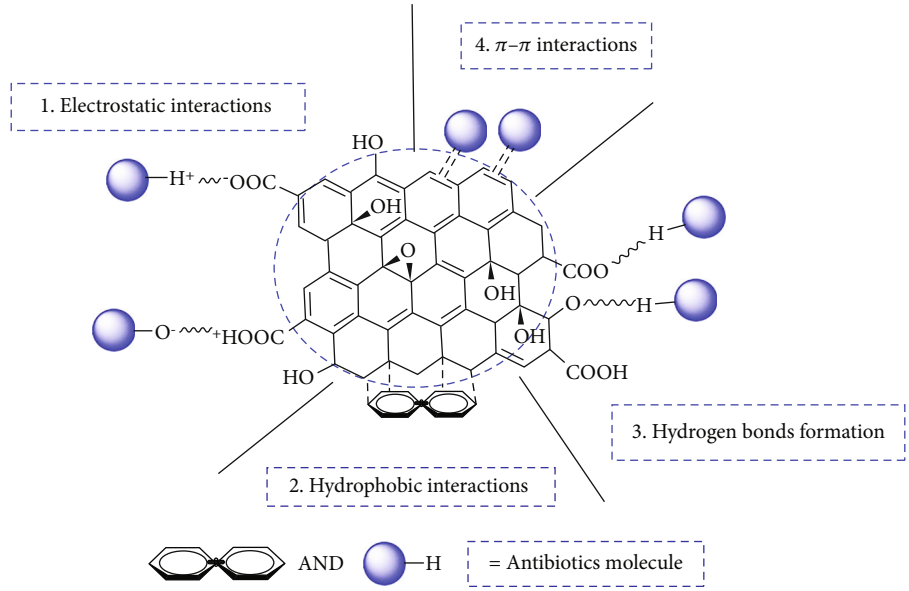

Figure 6: Adsorption mechanisms between carbon-based adsorbents and antibiotics. The types of adsorptive interaction include electrostatic interaction, hydrophobic interaction, hydrogen bond formation, and $\pi - \pi$ interaction.

inert gas. This is a single process wherein carbonisation and activation occur simultaneously. Important advantages of chemical over physical activation including the short activation time, well-controlled activation reaction, and consistently high surface area attainment. [3, 23] To date, the adsorptive removal of antibiotics by AC has been studied extensively.

6.1.1. Adsorptive Removal of Antibiotics by AC. Some researchers have incorporated nanoparticles into AC to enhance its adsorption capacity. Zhou et al. studied the adsorption behaviour of TC from an aqueous solution using powdered activated carbon (PAC) in association with ferro-ferric oxide nanoparticles (FONP-PAC). Scanning electron microscopy (SEM) images showed that the synthesised nanoparticles were well distributed on the surface, pores, and channels of the PAC, with an average particle size of 20–50 nm. However, FONP inside the pores of PAC reduced the surface area of the adsorbent, resulting in a mesoporous structure. The adsorption behaviours of 1FONP-PAC were also evaluated and determined to be pH-dependent. Electrostatic repulsion occurred between TC and 1FONP-PAC at high pH (>7.7), as both existed in anionic form, whereas low pH (<3.0) resulted in weak electrostatic interactions. 1FONP-PAC demonstrated the highest adsorption efficiency of 140.2 mg/g at pH 3. Isotherm and kinetic data showed that the adsorption process of 1FONP-PAC followed the Freundlich and Elovich kinetic models. Strong interactions between TC and the adsorbent were observed, as indicated by the separation factors ($1/n$) of 0.1456 and 0.0962 for 1FONP-PAC and PAC, respectively. Additionally, the adsorbent can be recycled from the aqueous solution using a magnetic field. After five cycles, the TC removal efficiency decreased from 98.78 to 52.71%, illustrating the regeneration potential of this adsorbent for future applications [59].

BC derived from pomelo peel and activated by potassium hydrochloride (KOH) was developed for the effective removal of TC from swine water. Increased pyrolytic temperatures increased the surface area and pore volume of BC. When activated by KOH, a significant enhancement of the surface area (2457.367 m^2/g) and pore volume (1.14 cm^3/g) of BC-KOH was observed by SEM analysis when compared with BC-400 and BC-600. The porous structure of the BC is closely related to its adsorption capacity, as BC-KOH exhibited the highest adsorption capacities of 124.95, 124.91, and 124.99 mg/g for TC, OTC, and CTC, respectively. However, when BC-KOH was tested in synthetic swine water, the removal efficiencies for TC, OTC, and CTC were 85.04, 82.17, and 96.64%, respectively. This indicated that other compounds in swine water affected the adsorption ability of the activated BC. The study found that a pseudo-second-order model was the best kinetic model, while the Langmuir model was the best isotherm model fitted to the adsorption. In addition, the highest adsorption capacity of the activated BC was obtained at pH 8.5, even though electrostatic repulsion occurred under these conditions. This indicated that besides electrostatic interactions, the possible adsorption mechanism of TCs onto the activated BC included $\pi - \pi$ interactions and pore filling. In addition to the adsorption characteristics, this study assessed the economic feasibility of BC-KOH for large-scale applications. The total cost per kilogram of BC-KOH (USD $9.82) was cheaper than the commercial AC (up to USD $45.71/kg). In addition, the temperature of 450–900°C and shorter chemical activation time resulted in low energy requirements for production and amenability for large-scale applications of BC-KOH [60].

Zhang et al. reported the performance of PAC for the removal of 28 antibiotics from water. Penicillin G (PNG), oxolinic acid (OLA), NDA, and flumequine (FMQ) were studied at an adsorbent dosage of 20 mg/L and contact time of 120 min. PAC exhibited excellent removal efficiency towards all the tested antibiotics where 96.5–99.9% and 86.8–99.6% of antibiotics were removed from deionized and surface waters, respectively. The decreased removal efficiency in surface waters could

be explained by the natural organic content competing with the antibiotics for PAC binding sites, and/or they may have interacted with the antibiotics and prevented them from approaching the pores. With increasing initial adsorbent concentration, the adsorption efficiency was enhanced. Increasing the adsorbent concentration results in a larger number of vacant active sites, enhancing the adsorption process. In terms of kinetics, the data fitted the best to the pseudo-second-order and Elovich models with R^2 values of >0.9989, indicating that chemisorption was dominant. In addition, the intercept (C value) from intraparticle diffusion did not pass through the origin, suggesting that intraparticle diffusion was not the only rate-limiting step of adsorption. In terms of isotherm studies, the Freundlich model fitted well with the adsorption data, implying multilayer adsorption on a heterogeneous surface [61].

Li et al. studied the removal of CIP using tea leave-derived biochar (UTC) under different conditions by altering the initial antibiotic concentration (150–500 mg/L), solution pH (4–10), and temperature (30–60°C). The adsorption capacity of CIP at equilibrium increased from 32.9 to 146.9 mg/g when the initial CIP concentration was increased from 150 to 200 mg/L. A greater concentration gradient between the aqueous and solid phases generates a stronger driving force for antibiotic transfer from the aqueous phase into the solid phase. The point of zero charge (pH_{pzc}) of UTC is 3.05, and at a higher pH, the adsorbent functional groups (-OH, -COOH, and -CN) become negatively charged through hydrogen ion release. CIP molecules containing carboxyl (pKa = 5.9) and amine (pKa = 8.8) groups were positively charged at pH < 5.9. Hence, a maximum adsorption of 78.24 mg/g was reported at pH 6, where CIP exists abundantly in its cationic form. The opposing charges of the adsorbent and antibiotic resulted in strong electrostatic interactions. The R^2 values indicate that both the Langmuir and Freundlich models fit well with the experimental data, and the adsorption process was concluded to be favourable, as the R_L value was 0.32 [62].

The removal of CIP and AMX was studied using *Prosopis juliflora*-derived AC (PPJ), showing maximum adsorption efficiencies at pH 4.0 and 7.0, respectively, with a higher adsorption capacity was observed for CIP. The PPJ surface was negatively charged at pH < 7.7. At pH 7.0, AMX exists as 60% zwitterions and 40% cations, which can interact with PPJ. In contrast, 99% of CIP was cationic at pH 4.0, allowing for a stronger affinity with PPJ-AC. Kinetic studies showed that adsorption followed a pseudo-second order, suggesting a chemical rate-limiting step. The data were investigated using the Langmuir, Freundlich, D-R, and Frumkin isotherm models. The Langmuir model with R^2 values of 0.97 and 0.99 for CIP and AMX, respectively, fitted the data best implying monolayer adsorption on a homogeneous surface. When adsorption was investigated in a binary system, AMX showed a cooperative effect on CIP adsorption. In contrast, CIP competitively affected AMX adsorption on PPJ. The used PPJ was regenerated using sodium hydroxide (NaOH) as antibiotics containing carboxylic salts were neutralised and desorbed. The adsorption efficiency was observed to reduce significantly from 98.55 to 47.75% (CIP) and 46.31 to 14.72% (AMX) after four regeneration cycles. The formation of sodium salts blocking the active sites and continuous morphology disruption of the active sites resulted in a lower efficiency [63].

Gholamiyan et al. produced AC derived from almond shells and used Fe_3O_4 nanoparticles to synthesise magnetic activated carbon (MAC) for the adsorptive removal of ERY. Based on the SEM images, Fe_3O_4 nanoparticles that imparted magnetic properties were evenly distributed on the surface of the MAC. Similar to previous studies, the adsorption of ERY by MAC was pH-dependent, with a pH_{pzc} of approximately 3.0 for the MAC hybrid. Electrostatic repulsion occurs at pH < 3.0, and the adsorption efficiency increases at pH > 3.0, owing to electrostatic attraction. The slight enhancement of adsorption (pH 3.0–5.2) could be explained by carbonyl and hydroxyl dehydration in ERY, leading to reduced activity of ERY under acidic conditions. As the pH was increased from 5.2 to 8.3, enhanced dehydration of ERY and stronger binding to active sites resulted in further increased adsorption. The maximum adsorption capacity of MAC was achieved at a pH of approximately 9.0, and response surface morphology was used to maximise the adsorption capacity. The maximum adsorption of 95.125% was achieved under optimal conditions, whereby the initial ERY concentration, MAC loading, temperature, and contact time were 65 mg/L, 1.55 g/L, 35°C, and 76.25 min, respectively. The adsorption isotherms and kinetics of MAC were investigated. The Freundlich isotherm and pseudo-second-order kinetic models showed the best agreement with the experimental data. Meanwhile, the Gibb's free energy change value was more negative with increasing temperature, indicating that the reaction is spontaneous and endothermic. MAC durability was evaluated in terms of stability and reusability of the adsorbent. No significant loss of adsorption sites was observed after five cycles, suggesting high stability and durability[64], and Table 2 summarises relevant studies.

6.2. Carbon Nanotubes. Carbon nanotubes (CNTs) have shown great potential as absorbents for water remediation.[65] CNTs are carbon allotropes with an aromatic surface that rolls up to form a cylindrical structure (Figure 5).[66] CNTs exhibit high mechanical strength, low electrical resistivity, and high thermal conductivity owing to their unique structure. [67] CNTs can be grouped into two main types based on the number of cylindrical shells: single-walled CNTs (SWCNTs) and multiwalled CNTs (MWCNTs). [68, 69] SWCNTs are cylindrical with a diameter of approximately 0.42 nm with a graphite wall ring at both ends. In contrast, MWCNTs are characterised by concentric cylinders with a layer-to-layer spacing of 0.34 nm and diameter that varies from 2 to 25 nm.[52] The site density, purity, surface area, porosity, functional groups, and CNT type determines their adsorption behaviour. CNTs usually cohere with each other and aggregate in aqueous solution via van der Waals interaction between raw CNTs forma large bundles. This limits their application for removing pollutants and antibiotics as they are difficult to disperse homogenously in most organic and aqueous solutions.[70] In general, CNTs can be functionalized (e.g., -COOH and -OH) via different methods to improve their adsorption ability and properties.[66, 71] [69] The unique structure and functional groups on CNT

Table 2: Antibiotics adsorption by activated carbon. The adsorptive characteristics of the adsorbents are summarised. ND: not determined.

Type of carbon-based adsorbent used	Antibiotics	Specific surface area (m^2/g)	pH_{pzc}	Optimal pH	Adsorption capacity (mg/g)/ removal efficiency (%)	Best-fitted isotherm model	References
Ferroferric oxide nanoparticles assisted powdered activated carbon, 1FON-PAC	TC	ND	ND	3.0	140.2/ND	Freundlich model and Elovich model	[59]
Pomelo peel derived biochar activated with KOH, BC-KOH	TC OTC CTC	2457.37	ND	6.5-7.5	476.19 /85.04 407.5/82.17 555.56/96.64	Langmuir model	[60]
Powdered activated carbon (PAC)	PNG OLA NDA FMQ	ND	ND	2.0-3.0	ND/96.2 ND/99.4 ND/98.4 ND/98.7	Freundlich model	[61]
Biochar derived from used tea leaves at different pyrolysis temperatures (350°C, 400°C, 450°C, 500°C, and 550°C), UTC	CIP	ND	3.05	6.0	238.10/ND	Langmuir and Freundlich model	[62]
Biochar derived from *Prosopis juliflora* wood, PPJ	CIP AMX	946.06	7.7	4.0 (CIP) 7.0 (AMX)	Single system: 250.00/ND (CIP) 714.29/ND (AMX) Binary System: 370.37/ND (CIP) 482.14/ND (AMX)	Langmuir model	[63]
Magnetic activated carbon (MAC)	ERY	941.48	3.0	9.0	248.909/95.125	Freundlich model	[64]

Table 3: Antibiotics adsorption by carbon nanotubes. The adsorptive characteristics of the adsorbents are summarised. ND: not determined.

Type of carbon-based adsorbent used	Antibiotics	Specific surface area (m^2/g)	Optimal pH	Adsorption capacity (mg/g)/ Removal efficiency (%)	Best-fitted isotherm model	References
Nanocomposite multiwalled carbon nanotube functionalized MIL-53(Fe)	TC OTC CTC	60.17	7.0	364.37/ND 325.59/ND 180.68/ND	Langmuir model	[70]
Ionic liquid-multiwalled carbon nanotubes, IL-MWCNTs composite tablet	TC	ND	ND	ND/99.76 ND/94.10 ND/84.60	Langmuir model	[71]
Single-walled carbon nanotube, SWCNT at different temperatures (273 K, 298 K, and 323 K)	AMX	ND	ND	108.84/ND 116.25/ND 122.48/ND	Langmuir model	[72]
Functionalized MWCNTs, CNT-2.0% O, CNT-3.2%O, CNT-4.7% O, and CNT-5.9%O	CIP	471 381 382 327	4	146.6/ND 168.6/ND 194.2/ND 176.2/ND	D-R model and Langmuir model	[75]
Multiwalled carbon nanotube, MWCNT	ERY	782.8	7.0	124.6/99.68	ND	[76]

surfaces allow them to interact with organic and inorganic compounds via different intermolecular forces.[66] Different CNT structures exhibit different adsorption processes because of the various available adsorption sites and variable access to adsorption sites.[72] In this regard, researchers have extensively studied the adsorptive removal of antibiotics by CNTs. CNT adsorbent characteristics and adsorption behaviour for antibiotics are summarised in Table 3.

6.2.1. Adsorptive Removal of Antibiotics by CNTs. Xiong et al. synthesised MWCNTs functionalized with MIL-53(Fe) and MWCNT/MIL-53(Fe) as adsorbents for antibiotic removal from aqueous solutions. A notable increase in the specific surface area and pore volume was observed when the MWCNTs were combined with MIL-53(Fe). Various mass ratios of MWCNT to MIL-53(Fe) in the composites (1, 5, 10, 20, and 30%) were synthesised, and MWCNT/MIL-53(Fe)-20% exhibited the greatest adsorption efficiency. This was attributed to the sharp increase in the pore volume, pore size, and surface area after MWCNT modification. The ionic strength and pH significantly influenced the adsorption ability where increased sodium chloride (NaCl) concentration resulted in decreased adsorption of TCs due to competition for active sites. In addition, reduced TC absorption was observed at higher pH, indicating electrostatic repulsion between the adsorbent and TCs. However, some TC adsorption was observed, illustrating that electrostatic interactions were not the only mechanism of adsorption, with others arising from $\pi - \pi$ stacking between the adsorbent and TC benzene ring, as well as the benzene ring electron cloud density-mediated adsorption. The highest adsorption capacity of MWCNT/MIL-53(Fe) was obtained at approximately pH 7.0, with values of 364.37, 325.59, and 180.68 mg/g for TC, OTC, and CTC, respectively. The kinetic adsorption data of TC, OTC, and CTC demonstrated the best agreement with the pseudo-second-order model, indicating that chemisorption occurred involving electron or valency force exchange between the adsorbent and TCs. The experimental data fitted better to the Langmuir isotherm model than to the Freundlich model. No major changes were observed in the efficiency of MWCNT/MIL-53(Fe) after reuse for four cycles, highlighting the stability and reusability of this adsorbent for TC removal [73].

Ionic liquid-multiwalled carbon nanotube (IL-MWCNT) composite tablets were synthesised by Chen et al. [74] for the removal of TCs and heavy metals. The ionic liquid, *N*-butyl benzothiazole hexafluorophosphate ($[C_4Bth][PF_6]$), was loaded into MWCNT. Ethyl cellulose was selected as the diluent to prepare the composite tablet as it could increase the compression stress to >15 MPa and is stable in water when compared to microcrystalline cellulose. The factors influencing the adsorptive removal of TCs by the IL-MWCNT composite tablets were investigated. At low pH, the electrostatic interaction between the anionic form of TCs and the positively charged adsorbent increased the adsorption efficiency, reaching a maximum removal of 98.53% at pH 4.5. At higher pH, the TCs existed predominantly in anionic form and the adsorption efficiency decreased because of electrostatic repulsion between the like charges of the adsorbent and adsorbate. TCs have no net charge at pH 3.3–7.7 and no significant decrease in removal efficiency (>96%) was observed in this pH range. This showed that besides electrostatic interactions, $\pi - \pi$ dispersion interactions between the TC molecules and the bulk π system on the MWCNT surface could be a major adsorption mechanism. In addition, adsorption increased with increasing temperature, indicating that the adsorption process was endothermic. Increasing temperature promoted TC trapping on the adsorbent, maximising the adsorption capacity at 99.76% at 40°C in 5 h. The pseudo-second-order kinetic model showed the best agreement with the experimental data, indicating that the adsorption rate was affected by intraparticle diffusion and external mass transfer. The best isotherm model was the Langmuir model, showing the involvement of single-

molecule adsorption. Importantly, the IL-MWCNT composite tablet achieved a desorption rate of >90%, and the adsorption efficiency decreased to <80% after three reuse cycles. The tablets were regenerated using an alkaline solution and reused until the adsorption efficiency was significantly reduced [68].

CNTs can be easily chemically modified to enhance their adsorption capacities.[65, 67] Therefore, hydroxylated (MH), carboxylated (MC), and graphitised (MG) MWCNTs were synthesised and compared with SWCNTs in terms of their CIP removal capacity.[69] SWCNTs with the highest surface area exhibited the highest adsorption capacity compared to the other modified MWCNTs. In addition, the optimum pH for CIP adsorption was 7.0 due to hydrophobic interactions, in agreement with the data reported by Ncibi and Sillanpaa.[75] However, while the hydrophobicity of MH was lower than that of MG owing to oxygen-containing functional group incorporation, the adsorption capacity of MH was higher than that of MG across all pH values, suggesting that other mechanisms contribute to the adsorption of CIP onto CNTs. FQ molecules can function as π-electron acceptors because of their electron-withdrawing fluorine groups and N-heteroaromatic rings. Thus, MH containing –OH groups acting as π-electron donors could interact with CIP via $\pi-\pi$ electron donor-acceptor interactions. In addition, electrostatic interactions were observed at a pH 4.0 to 6. The presence of hydrogen bond donors (–OH, C=O) in the antibiotics indicated the possibility of hydrogen bond formation with CNTs. The Freundlich model fitted well to the adsorption isotherm, and the n values obtained from the model ranged from 0.12 to 0.24, suggesting a heterogeneous adsorption energy distribution [69].

Using sodium hypochlorite as an oxidising agent, Yu et al. studied the adsorption potential of MWCNTs with oxygen contents ranging from 2.0 to 5.9%. Sodium hypochlorite introduced phenolic hydroxyl groups to the surface of the MWCNTs. Increasing the surface oxygen enhanced the hydrophilicity and dispersibility of the MWCNTs, resulting in improved CIP adsorption onto the active sites. However, excessive hydrophilicity inhibited adsorption owing to the formation of surface water clusters on the MWCNTs. MWCNTs with an oxygen content of 4.7% exhibited the highest adsorption capacity of 209.6 mg/g. A further increase in oxygen content was associated with a slower rate of increase in the maximum adsorption capacity. This decline was attributed to $\pi-\pi$ electron donor-acceptor interactions between the adsorbent and CIP. The phenolic hydroxyl groups on the MWCNT surface made the carbon ring a better π-electron donor, and the benzene ring linked to the fluorine atom of CIP is a good π-electron acceptor, resulting in $\pi-\pi$ electron donor-acceptor interactions. When the oxygen content increased from 4.7 to 5.9%, the phenolic hydroxyl content grew slower, leading to a decline in the adsorption capacity growth rate. Electrostatic interactions have been reported as the predominant adsorption mechanism. At pH 4.0, adsorption was facilitated by electrostatic attractions between the negatively charged CNTs-4.7%O and cationic CIP. The lowest adsorption was observed with electrostatic repulsion at pH 10, showing that the adsorption was strongly dependent on the physical and chemical properties of the MWCNTs. When the adsorption kinetics were investigated, the pseudo-second order fitted well with the experimental data, showing the importance of chemisorption. The experimental data were also fitted to the intraparticle diffusion model, showing that intraparticle diffusion was not the only rate-limiting step of the adsorption. Outer diffusion may also affect the adsorption rate and the D-R and Langmuir models best described the adsorption process. The average free energy of adsorption, E_a, calculated from the D-R model ranged from 1.78 to 3.97 kJ/mol, confirming the involvement of physisorption [76].

Balarak et al. investigated the effectiveness of SWCNTs for removing AMX. An increase in the initial AMX concentration resulted in an enhanced adsorption capacity and lowered adsorption efficiency. The lower adsorption efficiency was due to the lack of active sites available for the large number of AMX molecules in the concentrated solution. In contrast, increasing the SWCNT dose enhanced the adsorption efficiency owing to the large number of free active sites. However, the adsorption capacity was lower owing to the lack of active site saturation when the SWCNT dose increased and was related to the low ratio between the adsorbent and antibiotic. The adsorption of AMX could be completed within 45 min, removing 99% of the AMX at 323 K. When the SWCNT efficiency was studied at different temperatures, the maximum adsorption capacities at 278, 298, and 323 K were 108.84, 116.25, and 122.48 mg/g, respectively. The endothermic nature of the process was indicated by the increasing adsorption capacity with increasing temperature. The pseudo-second-order model described the adsorption well, with R^2 values ranging from 0.995 to 0.999 at different temperatures. The experimental data fitted better in the Langmuir model compared to the Freundlich model. The R_L values obtained from the Langmuir model ranged from zero to one, suggesting that the adsorption process was favourable regardless of temperature [67].

The effective removal of ERY from aqueous solutions by MWCNTs was reported by Mostafapour et al. Based on SEM and transmission electron microscopy (TEM), the main external and internal diameter of MWCNTs used were 2.0–3.5 and 1.2–1.7 nm, respectively, with a specific surface area of 782.8 m^2/g. The effects of contact time, temperature, mixing rate, and adsorbent dose on the adsorption ability towards ERY were investigated. A rapid increase in removal efficiency was observed during the first 30 min due to the large number of available active sites, followed by equilibrium at 75 min. When the temperature was increased, the removal efficiency increased, indicating that adsorption was endothermic. The highest removal efficiency (99.68%) and adsorption capacity (124.6 mg/g) were obtained at 318 K. The adsorption process exhibited a negative Gibbs free energy and positive entropy value, indicating that adsorption of ERY by MWCNTs is spontaneous with a high affinity for ERY. When the mixing rate was increased from 0 to 200 rpm, a significant increase in ERY adsorption efficiency was observed. The high mixing rate promoted contact between the adsorbent and ERY, increasing adsorption efficiency. An optimal removal of 98.9% was achieved at 200 rpm. Higher adsorbent dosages enhanced adsorption efficiency by providing more active sites, with an optimal dose of 1 g/L yielding a removal efficiency of 92.7%. A

further increase in the adsorbent dosage beyond 1 g/L resulted in negligible increases in adsorption capacity due to the saturation of the active sites. The adsorption kinetics followed a pseudo-second-order kinetic model, indicating chemisorption. Using the intraparticle diffusion model, both intraparticle and film diffusion were shown to control adsorption rates. The rate-determining step was further analysed using the Boyd kinetic model, showing that film diffusion limited the adsorption rate of ERY. The removal efficiency of ERY by MWCNTs was 99.4% under optimal conditions, suggesting that MWCNTs are promising adsorbents for ERY removal [77].

6.3. Graphene-Based Materials. Graphene is a two-dimensional single layer sp^2 hybridised carbon with a hexagonal aromatic ring structure (Figure 5). It is a promising adsorbent owing to its large surface area, electron-rich nature, electrostatic stacking properties, tunability with functional groups, and incorporation of multiple functional materials.[52] Graphene hydrophobicity allows it to interact with hydrophobic pollutants through van der Waals or $\pi - \pi$ interactions. However, hydrophobicity may also limit its application in aqueous media. Therefore, graphene is generally modified to produce graphene oxide (GO) or reduced graphene oxide (rGO).[52, 78] GO and rGO are chemically modified graphene materials that typically exhibit enhanced stability and dispersity compared to graphene. GO is produced by incorporating oxygen-containing functional groups, including carboxyl, hydroxyl, carbonyl, and epoxy groups. The presence of highly reactive functional groups on GO enables its application in aqueous environments owing to improved hydrophilicity. Removing some oxygen-containing functional groups on the surface of GO yields rGO. Sodium borohydride, ascorbic acid, and hydrazine are commonly used reducing reagents in the synthesis of rGO,[78] which shows improved photoactivity and electrical properties compared to unmodified graphene. The high surface area and large pore volume are attractive properties of rGO, which give rise to its high adsorption capability [52].

Graphene has a large surface area and high surface hydrophobicity which favours interactions with hydrophobic organic molecules. Surface modification of graphene can enhance its hydrophilicity and improve its ability to interact with a wider range of molecules. Researchers have combined nanomaterials with GO/rGO to further enhance their adsorption capacity for aqueous pollutants. Recently, interest in graphene-based nanomaterials has grown owing to their unique physicochemical properties, including high adsorption capacity, electroconductivity, good mechanical strength, and thermal stability. [74, 78] Metal oxide nanomaterials, including iron oxide and zirconium oxide, can enhance the removal efficiency for antibiotics.[79] Graphene-based materials can effectively treat water polluted with antibiotics as well as other organic and inorganic compounds.[80] Some innovative graphene-based adsorbents are reviewed in the following section.

6.3.1. Adsorptive Removal of Antibiotics by Graphene-Based Materials. Zou et al. composited α-Fe_2O_3 nanoparticles on rGO to form an α-Fe_2O_3/RGO hybrid sorbent for the removal of antibiotics (Table 4). The adsorptive capacities of α-Fe_2O_3/RGO-400 for TC, CTC, and OTC were determined to be 216.2, 180.8, and 98.4 mg/g, respectively, with adsorptive amounts of rGO for TC, CTC, and OTC of 102.1, 108.8, and 70.3 mg/g, respectively. This indicates that the α-Fe_2O_3 nanoparticles enhanced the adsorptive capability of rGO. In addition, the adsorption of TC and CTC was much higher than that of OTC, illustrating the relatively weak complexes formed between OTC and Fe(III). When tested at different pH values, the decontamination rate increased rapidly from pH 3.9 to 6.2 and decreased gradually when at pH > 9.2 for TC, with similar trends observed for CTC and OTC. This increased decontamination rate could be explained by weakened electrostatic repulsion as the pH was increased to near-neutral. As the pH increased to alkaline values (pH > 9.2), electrostatic repulsion between the TCs and adsorbent resulted in decreased decontamination rates. Approximately 85, 78, and 47% of the TC, CTC, and OTC were adsorbed within 20 min, without significant increases in decontamination rate after 30 min. Thus, a contact time of 30 min was sufficient for complete adsorption. The isotherm model followed the Langmuir isotherm model, while the adsorption kinetics of the TCs followed the pseudo-second-order model. The regeneration efficiency of α-Fe_2O_3/RGO was >90% for TC, CTC, and OTC after five cycles, illustrating the promising reusability of this hybrid sorbent for TC removal from aqueous solutions [79].

Miao et al. developed magnetic graphene oxide (MGO) to remove TCs (TC, CTC, and OTC) from aqueous solutions. The concentrations of TC, CTC, and OTC decreased rapidly in the first 400 min, followed by a gradual decrease, reaching a minimum concentration after approximately 8, 10, and 8 h, respectively. The increased adsorption capacity was mainly due to the high surface activity, large surface area, and full exposure of TCs to the MGO active sites. The maximum adsorption of TC, CTC, and OTC by MGO was 303.9514, 289.8551, and 141.4427 mg/g, respectively. For TC and OTC, the adsorption capacity increased from pH 2 to 7 and subsequently decreased at pH > 7. For CTC, a gradual increase in the adsorption capacity was observed from pH 2 to 7, followed by a rapid increase from pH 7 to 10. The difference in the adsorption capacity of MGO for TCs could be explained by the different ionic forms of TCs and changes in the zeta potential of MGO. The adsorption capacity increased with increasing temperature, indicating that adsorption was endothermic. Based on the isotherm and kinetic studies, the adsorption process fitted well to the Langmuir isotherm and pseudo-second-order kinetic models. After the adsorbent was reused for four cycles, the adsorption capacity decreased by approximately 25%. Further investigation using infrared spectroscopy showed the presence of an Fe-O absorption band, indicating that MGO retained its magnetic properties after being reused [81].

Zirconium oxide (ZrO_2) nanopowders with different structures, including monoclinic, tetragonal, and cubic, exhibited good performance for pollutant removal. Hao et al. developed nanocomposites of ZrO_2 and rGO, ZrO_2@rGO, consisting of pure monoclinic or tetragonal ZrO_2 to enhance the adsorptive removal of OTC. The m-ZrO_2@rGO and t-ZrO_2@rGO samples were prepared, and their adsorption performances were investigated. The adsorption capacity for OTC by t-ZrO_2@rGO (198.4 mg/g) was greater than m-ZrO_2@rGO (177.9 mg/g).

Table 4: Antibiotics adsorption by graphene and their oxides. The adsorptive characteristics of the adsorbents are summarised. ND: not determined.

Type of carbon-based adsorbent used	Antibiotics	Specific surface area (m^2/g)	pH_{pzc}	Optimal pH	Adsorption capacity (mg/g)	Best-fitted isotherm model	References
α-Iron oxide/reduced graphene oxide, α-Fe_2O_3/RGO nanocomposites	TC OTC CTC	281.9	ND	5.0-9.1	180.8 98.4 216.2	Langmuir model	[79]
Magnetic graphene oxide (MGO)	TC OTC CTC	ND	ND	3.3	303.9514 141.4427 289.8551	Langmuir model	[81]
monoclinic-ZrO2@rGO and tetragonal-ZrO_2@rGO	OTC	ND	7.4 and 7.6	4-8	177.9 198.4	Langmuir model	[82]
Graphene	CIP	1556	3.9	5-6	323	Freundlich model	[83]
Alkali-activated graphene, G-KOH	CIP	512.65	ND	8	177.6	Freundlich model	[84]
reduced graphene oxide/magnetite, RGO-M	CIP NOR	ND	2.7	5-7	12.22 22.20	Langmuir model	[85]

Both adsorbents showed a higher affinity towards OTC than TC or CTC due to the stronger complexation between OTC and ZrO_2 with a high Zr-OTC stability constant. The influence of the contact time and pH on OTC absorption by m-ZrO_2@rGO and t-ZrO_2@rGO was studied. Increased adsorption was observed at 0–20 min due to the abundant active sites available. Negligible increases were observed after 20 min, indicating that the system achieved adsorption equilibrium. At low pH (pH < 4), electrostatic repulsion between cationic OTC and the positively charged adsorbent surface hindered adsorption. With increasing pH from 4 to 8, the electrostatic attraction force, cation-π, $\pi - \pi$ stacking, and complexation enhanced OTC adsorption. Again, the electrostatic repulsion between OTC and the nanocomposites resulted in decreased adsorption at pH > 9. Further exploration of the adsorption mechanism between OTC and the nanocomposites revealed interaction via surface complexation. Complexation also affected the nanocomposite crystal structure. Isotherm analysis indicated that the Langmuir isotherm model best described OTC adsorption for both m-ZrO_2@rGO and t-ZrO_2@rGO. The kinetic study revealed that the pseudo-second-order model fitted the adsorptive kinetics well [82].

Zhu et al. compared the adsorption ability of graphene with coconut-derived GAC (CAC) for removing CIP and found that graphene outperformed CAC. The adsorption capacity of graphene was 323 mg/g, while CAC exhibited a maximum adsorption capacity of 217 mg/g. This can be explained by the greater specific surface area of graphene compared to CAC. In addition, up to 79.5% of the graphene pores were macropores. The large surface area and macropores facilitate the adsorption of macromolecules onto graphene active sites. The effect of the initial solution pH on CIP adsorption was investigated. When the pH was increased from 4 to 10, adsorption capacity decreased. Graphene existed in the negatively charged form in this range, with zero zeta potential at pH 3.9, whereas CIP was in cationic form below pH 6. At pH 6–8, CIP exists in the zwitterionic or neutral form. Therefore, when the pH increased, the interaction between graphene and CIP changed from electrostatic attraction to repulsion, rendering CIP adsorption less favourable. In addition to electrostatic interaction, shifting of the C=C bond absorption band in the Fourier transform infrared spectrum suggested a major role of $\pi - \pi$ interactions in the adsorption process. In the kinetic study, CIP adsorption by graphene fit better to the pseudo-second order compared to the pseudo-first order. This suggests that adsorption depends on active site availability and the adsorption capacities of the adsorbents were higher than the initial antibiotic concentrations. The CIP adsorption isotherm on graphene followed the Langmuir isotherm and the progressive saturation of graphene with increasing CIP concentration confirmed a monolayer adsorption process [83].

Yu et al. investigated the adsorption potential of alkali-activated graphene (G-KOH) for CIP removal. The adsorption capacity of G-KOH was higher than that of untreated graphene (G) by a factor of approximately 1.33 due to enhanced porosity and surface area. The surface area of G-KOH increased 3.7 times compared to that of graphene. The destruction of the graphitic structure of graphene after KOH treatment was responsible for the production of new micropores (0.056–0.209 cc/g), resulting in significant surface area increase. The oxygen atomic content of G-KOH increased after alkali activation treatment. The incorporation of oxygen-containing groups on the graphene surface promoted its dispersibility in aqueous solutions, exposed more active sites, and increased CIP adsorption. As CIP exists in different ionic forms at different pH values, the adsorption capacity varied over the tested pH range. At pH < 6 and > 8, the adsorption capacity decreased and remained unchanged at pH 6–8, consistent with the ionic forms of CIP at these pH values. The results showed that electrostatic interaction is the main controllable mechanism as the kinetic data of G-KOH fit well to the pseudo-second-order model. At a CIP concentration of 150 mg/L, equilibrium was reached after approximately 80 min. G-KOH fitted better to the Langmuir model whereas the Freundlich model fitted better for G adsorption. The calculated E value from the D-R

model was <5 kJ/mol, revealing that physical adsorption was the predominant mechanism between the CIP and adsorbents [84].

The applicability of graphene-based materials in aqueous solutions can be improved by combining graphene, GO, or rGO with inorganic composite materials. Theoretically, the addition of magnetite can allow for easier retrieval of used adsorbents after treatment using a magnet, avoiding the need for centrifugation or filtration. Tang et al. synthesised an rGO/magnetite composite (RGO-M) in situ and investigated its adsorption capability for CIP and NOR. The surface morphology revealed that the monodispersed Fe_3O_4 microspheres were distributed homogeneously on the rGO surface, with an average diameter of approximately 130 nm. An absorption band at approximately 1440 cm^{-1} was observed in the infrared spectrum, indicating complex formation between the carboxyl functional group and Fe on the magnetic particles. This indicates that the Fe_3O_4 microspheres were covalently bonded to rGO. At room temperature (298 K) and pH 6.2, the maximum adsorption capacities were 18.22 and 22.20 mg/g for CIP and NOR, respectively. The adsorption was well described by the pseudo-second-order and Langmuir models. In addition, a good fit to the Temkin model illustrates the role of electrostatic interactions during adsorption. The involvement of electrostatic interactions was further confirmed when the electrostatic repulsion reduced the adsorption capacity at higher pH. In contrast, $\pi - \pi$ and hydrophobic interactions dominated the adsorption process at pH 5.0 to 7.0, where the antibiotics predominately exist in zwitterionic forms.[85] Table 4 summarises relevant studies regarding the antibiotic removal by graphene-based materials.

7. Conclusions

Although antibiotics can improve public health and quality of life, their presence in the environment poses potential threats to human health. With rapid societal development, conventional activated carbon and graphene-based materials have demonstrated that carbonaceous materials can play an important role in the adsorptive removal of antibiotics. Activated carbon is the most commonly used adsorbent, but its adsorption capacity and selectivity can be further improved. Carbon nanotubes and graphene exhibit good adsorption capacities and have been widely applied to construct advanced adsorbents for antibiotic removal from aqueous solutions.

Although adsorption is an effective method for combating antibiotic pollution, a few limitations must be addressed to produce a better adsorbent.

(1) High production and regeneration costs often limit the commercial application of ACs, CNTs, and graphene

(2) Disposal of secondary waste, including spent adsorbent and recovered antibiotics, remains a challenge

(3) Potential secondary pollution from carbon adsorbents modified with metals

In addition, most experiments were conducted under laboratory conditions wherein the antibiotic solutions are prepared without interferents, resulting in discrepancies when the adsorbent is applied to actual wastewater. Therefore, more concerted efforts are needed to produce practical, green, stable, and economically feasible carbonaceous adsorbents for antibiotic removal from aquatic environments.

Conflicts of Interest

The authors declare no conflicts of interest regarding the publication of this article.

Acknowledgments

This work was supported by the International Medical University under grant BP I-01-2021(09).

References

[1] H. Fu, X. Li, J. Wang et al., "Activated carbon adsorption of quinolone antibiotics in water: performance, mechanism, and modeling," *Journal of Environmental Sciences*, vol. 1, no. 56, pp. 145–152, 2017.

[2] J. Ma, Z. Jiang, J. Cao, and F. Yu, "Enhanced adsorption for the removal of antibiotics by carbon nanotubes/graphene oxide/sodium alginate triple-network nanocomposite hydrogels in aqueous solutions," *Chemosphere*, vol. 1, no. 242, article 125188, 2020.

[3] F. Yu, Y. Li, S. Han, and J. Ma, "Adsorptive removal of antibiotics from aqueous solution using carbon materials," *Chemosphere*, vol. 1, no. 153, pp. 365–385, 2016.

[4] B. L. Phoon, C. C. Ong, M. S. Mohamed Saheed et al., "Conventional and emerging technologies for removal of antibiotics from wastewater," *Journal of Hazardous Materials*, vol. 5, no. 400, article 122961, 2020.

[5] X. S. Miao, F. Bishay, M. Chen, and C. D. Metcalfe, "Occurrence of antimicrobials in the final effluents of wastewater treatment plants in Canada," *Environmental Science & Technology*, vol. 38, no. 13, pp. 3533–3541, 2004.

[6] M. E. Lindsey, M. Meyer, and E. M. Thurman, "Analysis of trace levels of sulfonamide and tetracycline antimicrobials in groundwater and surface water using solid-phase extraction and liquid chromatography/mass spectrometry," *Analytical Chemistry*, vol. 73, no. 19, pp. 4640–4646, 2001.

[7] K. G. Karthikeyan and M. T. Meyer, "Occurrence of antibiotics in wastewater treatment facilities in Wisconsin, USA," *Science of the Total Environment*, vol. 361, no. 1–3, pp. 196–207, 2006.

[8] S. Rodriguez-Mozaz, I. Vaz-Moreira, S. V. Della Giustina et al., "Antibiotic residues in final effluents of European wastewater treatment plants and their impact on the aquatic environment," *Environment International*, vol. 1, no. 140, article 105733, 2020.

[9] R. H. Lindberg, P. Wennberg, M. I. Johansson, M. Tysklind, and A. Bav, "Screening of human antibiotic substances and determination of weekly mass flows in five sewage treatment plants in Sweden," *Environmental Science & Technology*, vol. 39, no. 10, pp. 3421–3429, 2005.

[10] D. W. Kolpin, E. T. Furlong, M. T. Meyer et al., "Pharmaceuticals, hormones, and other organic wastewater contaminants in U.S. streams, 1999–2000: a national reconnaissance," *Environmental Science & Technology*, vol. 36, no. 6, pp. 1202–1211, 2002.

[11] M. A. F. Locatelli, F. F. Sodré, and W. F. Jardim, "Determination of antibiotics in Brazilian surface waters using liquid chromatography-electrospray tandem mass spectrometry," *Archives of Environmental Contamination and Toxicology*, vol. 60, no. 3, pp. 385–393, 2011.

[12] R. Mirzaei, M. Yunesian, S. Nasseri et al., "Occurrence and fate of most prescribed antibiotics in different water environments of Tehran, Iran," *Science of the Total Environment*, vol. 619–620, pp. 446–459, 2018.

[13] S. Castiglioni, F. Pomati, K. Miller et al., "Novel homologs of the multiple resistance regulator marA in antibiotic-contaminated environments," *Water Research*, vol. 42, no. 16, pp. 4271–4280, 2008.

[14] F. Tamtam, F. Mercier, B. Le Bot et al., "Occurrence and fate of antibiotics in the Seine River in various hydrological conditions," *Science of the Total Environment*, vol. 393, no. 1, pp. 84–95, 2008.

[15] T. aus der Beek, F. A. Weber, A. Bergmann et al., "Pharmaceuticals in the environment—global occurrences and perspectives," *Environmental Toxicology and Chemistry*, vol. 35, no. 4, pp. 823–835, 2016.

[16] Q. Tuc Dinh, F. Alliot, E. Moreau-Guigon, J. Eurin, M. Chevreuil, and P. Labadie, "Measurement of trace levels of antibiotics in river water using on-line enrichment and triple-quadrupole LC-MS/MS," *Talanta*, vol. 85, no. 3, pp. 1238–1245, 2011.

[17] N. Hanna, P. Sun, Q. Sun et al., "Presence of antibiotic residues in various environmental compartments of Shandong province in eastern China: its potential for resistance development and ecological and human risk," *Environment International*, vol. 1, no. 114, pp. 131–142, 2018.

[18] M. C. Danner, A. Robertson, V. Behrends, and J. Reiss, "Antibiotic pollution in surface fresh waters: occurrence and effects," *Science of the Total Environment*, vol. 10, no. 664, pp. 793–804, 2019.

[19] F. Ahmad, D. Zhu, and J. Sun, "Environmental fate of tetracycline antibiotics: degradation pathway mechanisms, challenges, and perspectives," *Environmental Sciences Europe*, vol. 33, no. 1, pp. 1–17, 2021.

[20] J. Lyu, L. Yang, L. Zhang, B. Ye, and L. Wang, "Antibiotics in soil and water in China–a systematic review and source analysis," *Environmental Pollution*, vol. 1, no. 266, article 115147, 2020.

[21] K. Li, J. J. Li, N. Zhao, Y. Ma, and B. Di, "Removal of tetracycline in sewage and dairy products with high-stable MOF," *Molecules*, vol. 25, no. 6, 2020.

[22] G. Gopal, S. A. Alex, N. Chandrasekaran, and A. Mukherjee, "A review on tetracycline removal from aqueous systems by advanced treatment techniques," *RSC Advances*, vol. 10, no. 45, pp. 27081–27095, 2020.

[23] M. J. Ahmed, "Adsorption of quinolone, tetracycline, and penicillin antibiotics from aqueous solution using activated carbons: review," *Environmental Toxicology and Pharmacology*, vol. 1, no. 50, pp. 1–10, 2017.

[24] E. L. Thiang, C. W. Lee, H. Takada et al., "Antibiotic residues from aquaculture farms and their ecological risks in Southeast Asia: a case study from Malaysia," *Ecosystem Health and Sustainability*, vol. 7, no. 1, 2021.

[25] D. E. King, R. Malone, and S. H. Lilley, "New classification and update on the quinolone antibiotics," *American Family Physician*, vol. 61, no. 9, pp. 2741–2748, 2000.

[26] T. D. M. Pham, Z. M. Ziora, and M. A. T. Blaskovich, "Quinolone antibiotics," *Medchemcomm*, vol. 10, no. 10, pp. 1719–1739, 2019.

[27] H. Q. Anh, D. L. N. Tp, X. X. Lu et al., "Antibiotics in surface water of East and Southeast Asian countries: a focused review on contamination status, pollution sources, potential risks, and future perspectives," *Science of The Total Environment*, vol. 764, 2021.

[28] M. Lobanovska and G. Pilla, "Penicillin's discovery and antibiotic resistance: lessons for the future?," *The Yale Journal of Biology and Medicine*, vol. 90, no. 1, pp. 135–145, 2017.

[29] A. J. Sorinolu, N. Tyagi, A. Kumar, and M. Munir, "Antibiotic resistance development and human health risks during wastewater reuse and biosolids application in agriculture," *Chemosphere*, vol. 265, article 129032, 2021.

[30] Z. Yan, X. Huang, Y. Xie, M. Song, K. Zhu, and S. Ding, "Macrolides induce severe cardiotoxicity and developmental toxicity in zebrafish embryos," *Science of the Total Environment*, vol. 1, no. 649, pp. 1414–1421, 2019.

[31] I. Senta, S. Terzic, and M. Ahel, "Analysis and occurrence of macrolide residues in stream sediments and underlying alluvial aquifer downstream from a pharmaceutical plant," *Environmental Pollution*, vol. 15, no. 273, article 116433, 2021.

[32] I. Senta, P. Kostanjevecki, I. Krizman-Matasic, S. Terzic, and M. Ahel, "Occurrence and behavior of macrolide antibiotics in municipal wastewater treatment: possible importance of metabolites, synthesis byproducts, and transformation products," *Environmental Science & Technology*, vol. 53, no. 13, pp. 7463–7472, 2019.

[33] Y. Dai, M. Liu, J. Li et al., "A review on pollution situation and treatment methods of tetracycline in groundwater," *Separation Science and Technology*, vol. 55, no. 5, pp. 1005–1021, 2020.

[34] N. Wang, X. Hang, M. Zhang, X. Liu, and H. Yang, "Analysis of newly detected tetracycline resistance genes and their flanking sequences in human intestinal bifidobacteria," *Scientific Reports*, vol. 7, no. 1, pp. 1–10, 2017.

[35] S. I. Polianciuc, A. E. Gurzău, B. Kiss, M. Georgia Ștefan, and F. Loghin, "Antibiotics in the environment: causes and consequences," *Medicine and Pharmacy Reports*, vol. 93, no. 3, pp. 231–240, 2020.

[36] M. Lillenberg, S. V. Litvin, L. Nei, M. Roasto, and K. Sepp, "Enrofloxacin and ciprofloxacin uptake by plants from soil," *Agronomy Research*, vol. 8, no. 1, pp. 807–814, 2010.

[37] A. E. Pérez-Cobas, M. J. Gosalbes, A. Friedrichs et al., "Gut microbiota disturbance during antibiotic therapy: a multi-omic approach," *Gut*, vol. 62, no. 11, pp. 1591–1601, 2013.

[38] Y. Ben, C. Fu, M. Hu, L. Liu, M. H. Wong, and C. Zheng, "Human health risk assessment of antibiotic resistance associated with antibiotic residues in the environment: a review," *Environmental Research*, vol. 169, pp. 483–493, 2019.

[39] M. Milaković, G. Vestergaard, J. J. González-Plaza et al., "Pollution from azithromycin-manufacturing promotes macrolide-resistance gene propagation and induces spatial and seasonal bacterial community shifts in receiving river sediments," *Environment International*, vol. 1, no. 123, pp. 501–511, 2019.

[40] D. L. Cheng, H. H. Ngo, W. S. Guo et al., "Bioprocessing for elimination antibiotics and hormones from swine wastewater," *Science of the Total Environment*, vol. 15, no. 621, pp. 1664–1682, 2018.

[41] Z. Y. Lu, Y. L. Ma, J. T. Zhang, N. S. Fan, B. C. Huang, and R. C. Jin, "A critical review of antibiotic removal strategies:

performance and mechanisms," *Journal of Water Process Engineering*, vol. 38, article 101681, 2020.

[42] D. Cheng, H. H. Ngo, W. Guo et al., "A critical review on antibiotics and hormones in swine wastewater: water pollution problems and control approaches," *Journal of Hazardous Materials*, vol. 5, no. 387, article 121682, 2020.

[43] R. K. Langbehn, C. Michels, and H. M. Soares, "Antibiotics in wastewater: from its occurrence to the biological removal by environmentally conscious technologies," *Environmental Pollution*, vol. 15, no. 275, article 116603, 2021.

[44] B. Tiwari, B. Sellamuthu, Y. Ouarda, P. Drogui, R. D. Tyagi, and G. Buelna, "Review on fate and mechanism of removal of pharmaceutical pollutants from wastewater using biological approach," *Bioresource Technology*, vol. 1, no. 224, pp. 1–12, 2017.

[45] A. S. Oberoi, Y. Jia, H. Zhang, S. K. Khanal, and H. Lu, "Insights into the fate and removal of antibiotics in engineered biological treatment systems: a critical review," *Environmental Science & Technology*, vol. 53, no. 13, pp. 7234–7264, 2019.

[46] M. N. Chollom, S. Rathilal, F. M. Swalaha, B. F. Bakare, and E. K. Tetteh, "Removal of antibiotics during the anaerobic digestion of slaughterhouse wastewater," *International Journal of Sustainable Development and Planning*, vol. 15, no. 3, pp. 335–343, 2020.

[47] V. Homem and L. Santos, "Degradation and removal methods of antibiotics from aqueous matrices - a review," *Journal of Environmental Management*, vol. 92, no. 10, pp. 2304–2347, 2011.

[48] S. Navalon, M. Alvaro, and H. Garcia, "Reaction of chlorine dioxide with emergent water pollutants: product study of the reaction of three β-lactam antibiotics with ClO2," *Water Research*, vol. 42, no. 8–9, pp. 1935–1942, 2008.

[49] V. K. Sharma, "Oxidative transformations of environmental pharmaceuticals by Cl2, ClO2, O3, and Fe(VI): kinetics assessment," *Chemosphere*, vol. 73, no. 9, pp. 1379–1386, 2008.

[50] M. M. Huber, S. Korhonen, T. A. Ternes, and U. Von Gunten, "Oxidation of pharmaceuticals during water treatment with chlorine dioxide," *Water Research*, vol. 39, no. 15, pp. 3607–3617, 2005.

[51] J. Dutta and A. A. Mala, "Removal of antibiotic from the water environment by the adsorption technologies: a review," *Water Science and Technology*, vol. 82, no. 3, pp. 401–426, 2020.

[52] Y. Xiang, Z. Xu, Y. Wei et al., "Carbon-based materials as adsorbent for antibiotics removal: mechanisms and influencing factors," *Journal of Environmental Management*, vol. 1, no. 237, pp. 128–138, 2019.

[53] D. Dassharma, S. Samanta, S. Dharun Nithish Kumar, and G. Halder, "A mechanistic insight into enrofloxacin sorptive affinity of chemically activated carbon engineered from green coconut shell," *Journal of Environmental Chemical Engineering*, vol. 8, no. 5, article 104140, 2020.

[54] A. Chandrasekaran, C. Patra, S. Narayanasamy, and S. Subbiah, "Adsorptive removal of ciprofloxacin and amoxicillin from single and binary aqueous systems using acid-activated carbon from Prosopis juliflora," *Environmental Research*, vol. 188, article 109825, 2020.

[55] L. Limousy, I. Ghouma, A. Ouederni, and M. Jeguirim, "Amoxicillin removal from aqueous solution using activated carbon prepared by chemical activation of olive stone," *Environmental Science and Pollution Research*, vol. 24, no. 11, pp. 9993–10004, 2017.

[56] A. Yazidi, M. Atrous, F. Edi Soetaredjo et al., "Adsorption of amoxicillin and tetracycline on activated carbon prepared from durian shell in single and binary systems: experimental study and modeling analysis. Chem," *Chemical Engineering Journal*, vol. 379, article 122320, 2020.

[57] H. S. Kambo and A. Dutta, "A comparative review of biochar and hydrochar in terms of production, physico-chemical properties and applications," *Renewable and Sustainable Energy Reviews*, vol. 45, pp. 359–378, 2015.

[58] J. Fang, L. Zhan, Y. S. Ok, and B. Gao, "Minireview of potential applications of hydrochar derived from hydrothermal carbonization of biomass," *Journal of Industrial and Engineering Chemistry*, vol. 57, pp. 15–21, 2018.

[59] J. Zhou, F. Ma, and H. Guo, "Adsorption behavior of tetracycline from aqueous solution on ferroferric oxide nanoparticles assisted powdered activated carbon," *Chemical Engineering Journal*, vol. 15, no. 384, article 123290, 2020.

[60] D. Cheng, H. H. Ngo, W. Guo et al., "Feasibility study on a new pomelo peel derived biochar for tetracycline antibiotics removal in swine wastewater," *Science of the Total Environment*, vol. 720, article 137662, 2020.

[61] X. Zhang, W. Guo, H. H. Ngo, H. Wen, N. Li, and W. Wu, "Performance evaluation of powdered activated carbon for removing 28 types of antibiotics from water," *Journal of Environmental Management*, vol. 172, pp. 193–200, 2016.

[62] D. G. Kim, D. Choi, S. Cheon, S. O. Ko, S. Kang, and S. Oh, "Addition of biochar into activated sludge improves removal of antibiotic ciprofloxacin," *Journal of Water Process Engineering*, vol. 33, article 101019, 2020.

[63] J. Li, G. Yu, L. Pan et al., "Study of ciprofloxacin removal by biochar obtained from used tea leaves," *Journal of Environmental Sciences (China)*, vol. 73, pp. 20–30, 2018.

[64] S. Gholamiyan, M. Hamzehloo, and A. Farrokhnia, "RSM optimized adsorptive removal of erythromycin using magnetic activated carbon: adsorption isotherm, kinetic modeling and thermodynamic studies," *Sustainable Chemistry and Pharmacy*, vol. 1, no. 17, article 100309, 2020.

[65] J. Ahmad, S. Naeem, M. Ahmad, A. R. A. Usman, and M. I. Al-Wabel, "A critical review on organic micropollutants contamination in wastewater and removal through carbon nanotubes," *Journal of Environmental Management*, vol. 246, pp. 214–228, 2019.

[66] M. Bassyouni, A. E. Mansi, A. Elgabry, B. A. Ibrahim, O. A. Kassem, and R. Alhebeshy, "Utilization of carbon nanotubes in removal of heavy metals from wastewater: a review of the CNTs' potential and current challenges," *Applied Physics A*, vol. 126, no. 1, pp. 1–33, 2019.

[67] D. Balarak, Y. Mahdavi, A. Maleki, H. Daraei, and S. Sadeghi, "Studies on the removal of amoxicillin by single walled carbon nanotubes," *British Journal of Pharmaceutical Research*, vol. 10, no. 4, pp. 1–9, 2016.

[68] C. Chen, X. Feng, and S. Yao, "Ionic liquid-multi walled carbon nanotubes composite tablet for continuous adsorption of tetracyclines and heavy metals," *Journal of Cleaner Production*, vol. 1, no. 286, article 124937, 2021.

[69] H. Li, D. Zhang, X. Han, and B. Xing, "Adsorption of antibiotic ciprofloxacin on carbon nanotubes: PH dependence and thermodynamics," *Chemosphere*, vol. 95, pp. 150–155, 2014.

[70] L. Ouni, A. Ramazani, and S. Taghavi Fardood, "An overview of carbon nanotubes role in heavy metals removal from

wastewater," *Frontiers of Chemical Science and Engineering*, vol. 13, no. 2, pp. 274–295, 2019.

[71] F. Mashkoor and A. Nasar, "Carbon nanotube-based adsorbents for the removal of dyes from waters: a review," *Environmental Chemistry Letters*, vol. 18, no. 3, pp. 605–629, 2020.

[72] S. A. Mousavi and H. Janjani, "Antibiotics adsorption from aqueous solutions using carbon nanotubes: a systematic review," *Toxin Reviews*, vol. 39, no. 2, pp. 87–98, 2018.

[73] W. Xiong, G. Zeng, Z. Yang et al., "Adsorption of tetracycline antibiotics from aqueous solutions on nanocomposite multi-walled carbon nanotube functionalized MIL-53(Fe) as new adsorbent," *Science of the Total Environment*, vol. 15, no. 627, pp. 235–244, 2018.

[74] A. C. Sophia, E. C. Lima, N. Allaudeen, and S. Rajan, "Application of graphene based materials for adsorption of pharmaceutical traces from water and wastewater- a review," *Desalination and Water Treatment*, vol. 57, no. 57, pp. 27573–27586, 2016.

[75] M. C. Ncibi and M. Sillanpää, "Optimized removal of antibiotic drugs from aqueous solutions using single, double and multi-walled carbon nanotubes," *Journal of Hazardous Materials*, vol. 298, pp. 102–110, 2015.

[76] F. Yu, S. Sun, S. Han, J. Zheng, and J. Ma, "Adsorption removal of ciprofloxacin by multi-walled carbon nanotubes with different oxygen contents from aqueous solutions," *Chemical Engineering Journal*, vol. 285, pp. 588–595, 2016.

[77] F. K. Mostafapour, M. Dashtizade, and D. Balarak, "Adsorption thermodynamics, kinetics and mechanism for the adsorption of erythromycin onto multi-walled carbon nanotubes," *Journal of Pharmaceutical Research International*, vol. 24, no. 6, pp. 1–11, 2018.

[78] X. Wang, R. Yin, L. Zeng, and M. Zhu, "A review of graphene-based nanomaterials for removal of antibiotics from aqueous environments," *Environmental Pollution*, vol. 1, no. 253, pp. 100–110, 2019.

[79] S. J. Zou, Y. F. Chen, Y. Zhang, X. F. Wang, N. You, and H. T. Fan, "A hybrid sorbent of α-iron oxide/reduced graphene oxide: studies for adsorptive removal of tetracycline antibiotics," *Journal of Alloys and Compounds*, vol. 15, no. 863, article 158475, 2021.

[80] M. F. Li, Y. G. Liu, G. M. Zeng, N. Liu, and S. B. Liu, "Graphene and graphene-based nanocomposites used for antibiotics removal in water treatment: a review," *Chemosphere*, vol. 1, no. 226, pp. 360–380, 2019.

[81] J. Miao, F. Wang, Y. Chen, Y. Zhu, Y. Zhou, and S. Zhang, "The adsorption performance of tetracyclines on magnetic graphene oxide: a novel antibiotics absorbent," *Applied Surface Science*, vol. 1, no. 475, pp. 549–558, 2019.

[82] D. Hao, Y. X. Song, Y. Zhang, and H. T. Fan, "Nanocomposites of reduced graphene oxide with pure monoclinic-ZrO2 and pure tetragonal-ZrO2 for selective adsorptive removal of oxytetracycline," *Applied Surface Science*, vol. 30, no. 543, article 148810, 2021.

[83] X. Zhu, D. C. W. Tsang, F. Chen, S. Li, and X. Yang, "Ciprofloxacin adsorption on graphene and granular activated carbon: kinetics, isotherms, and effects of solution chemistry," *Environmental Technology*, vol. 36, no. 24, pp. 3094–3102, 2015.

[84] F. Yu, J. Ma, and D. Bi, "Enhanced adsorptive removal of selected pharmaceutical antibiotics from aqueous solution by activated graphene," *Environmental Science and Pollution Research*, vol. 22, no. 6, pp. 4715–4724, 2015.

[85] Y. Tang, H. Guo, L. Xiao, S. Yu, N. Gao, and Y. Wang, "Synthesis of reduced graphene oxide/magnetite composites and investigation of their adsorption performance of fluoroquinolone antibiotics," *Colloids and Surfaces A: Physicochemical and Engineering Aspects*, vol. 424, pp. 74–80, 2013.